

## **SUPPLEMENTARY INFORMATION**

### **SUPPLEMENTARY MATERIAL AND METHODS**

#### **Antibodies**

The following primary antibodies were used: anti-LRP4 (rabbit polyclonal, Atlas prestige antibodies HPA012300, Sigma Aldrich, Hamburg, Germany); anti-LRP4 (rabbit polyclonal, raised against the intracellular part of the protein, amino acids: 1755-1905; (Zhang, et al., 2015; Choi, et al., 2013). Both antibodies were affinity-purified and gave similar results in Western blotting and immunochemistry. We observed no staining with either antibody in muscle tissue from E18.5 LRP4 knockout mice, demonstrating their specificity (data not shown). Moreover, pre-incubation of the antibodies with an excess of the protein used for immunization abolished the staining of CNS tissue sections (data not shown). Anti-LRP4 (mouse monoclonal IgG2a, NeuroMab, Davis, California); anti- $\alpha$ -tubulin (mouse monoclonal IgG1, Sigma); anti- $\beta$ -actin (mouse monoclonal IgG, Cell Signaling); anti-MAP2 (mouse monoclonal IgG1, Sigma); anti- $\alpha$ -CamKII (mouse monoclonal IgG1, Abcam, Cambridge, UK); anti-GABA (rabbit polyclonal, Sigma); anti-GFP (chicken polyclonal, Abcam); anti-bassoon (rabbit polyclonal, generously provided by Wilko Altmann, Magdeburg, Germany; (Zhang, et al., 2015); anti-PSD95 (mouse monoclonal IgG2a, Thermo Fisher Scientific, Nidderau, Germany); anti-Synaptobrevin2 (mouse monoclonal IgG1, Synaptic Systems, Göttingen, Germany); anti-RFP (rat monoclonal IgG2a, Chromotek, Planegg-Martinsried, Germany); anti-agrin (rabbit polyclonal against the C-terminal 95 kDa fragment, detects all isoforms of agrin and reacts with TM-agrin as well as with NtA-agrin (Eusebio, et al., 2003); anti-mCherry (goat polyclonal; Acris Antibodies, Herford, Germany); anti- $\beta$ III tubulin (mouse monoclonal IgG2b, Sigma); anti-Tau (mouse monoclonal IgG2a, Millipore); anti-CTIP2 (rat monoclonal IgG2a, Abcam). As

secondary antibodies, we used highly pre-absorbed, Alexa-conjugated antibodies directed against the appropriate species and monoclonal isotype (Alexa 488, 594 and 647, Invitrogen, Darmstadt, Germany) as well as HRP-conjugated goat antibodies (Invitrogen).

### **Preparation of protein lysates and Western blotting**

The cultures were lysed in RIPA buffer (10 mM Na<sub>2</sub>HPO<sub>4</sub>, pH 7.2, 150 mM NaCl, 1% sodium deoxicolate, 1% Nonidet P-40, 0.1% SDS) containing protease (Complete EDTA-free, Roche). Protein concentrations were determined with the BCA reagent from Interchim. Equal amounts of protein (50 µg) were diluted in Laemmli Sample buffer containing β-mercaptoethanol (BioRad, 161-0747) and separated by polyacrylamide gel electrophoresis and transferred to polyvinylidene difluoride membranes (Pall; Life Sciences). Immunodetection of proteins was performed by standard procedures (ECL Prime Western Blotting Detection Reagent, Amersham).

### **Time-lapse imaging of dissociated cortical neuronal cultures**

Time-lapse video microscopy of cortical neuronal cultures was performed as previously described (Costa, et al., 2008). Phase contrast and fluorescent images were acquired every 10 or 20 min, respectively. Single-neurite tracing was performed in ImageJ using the Simple Neurite Tracer plugin (Longair, et al., 2011).

### **Electrophysiological recordings**

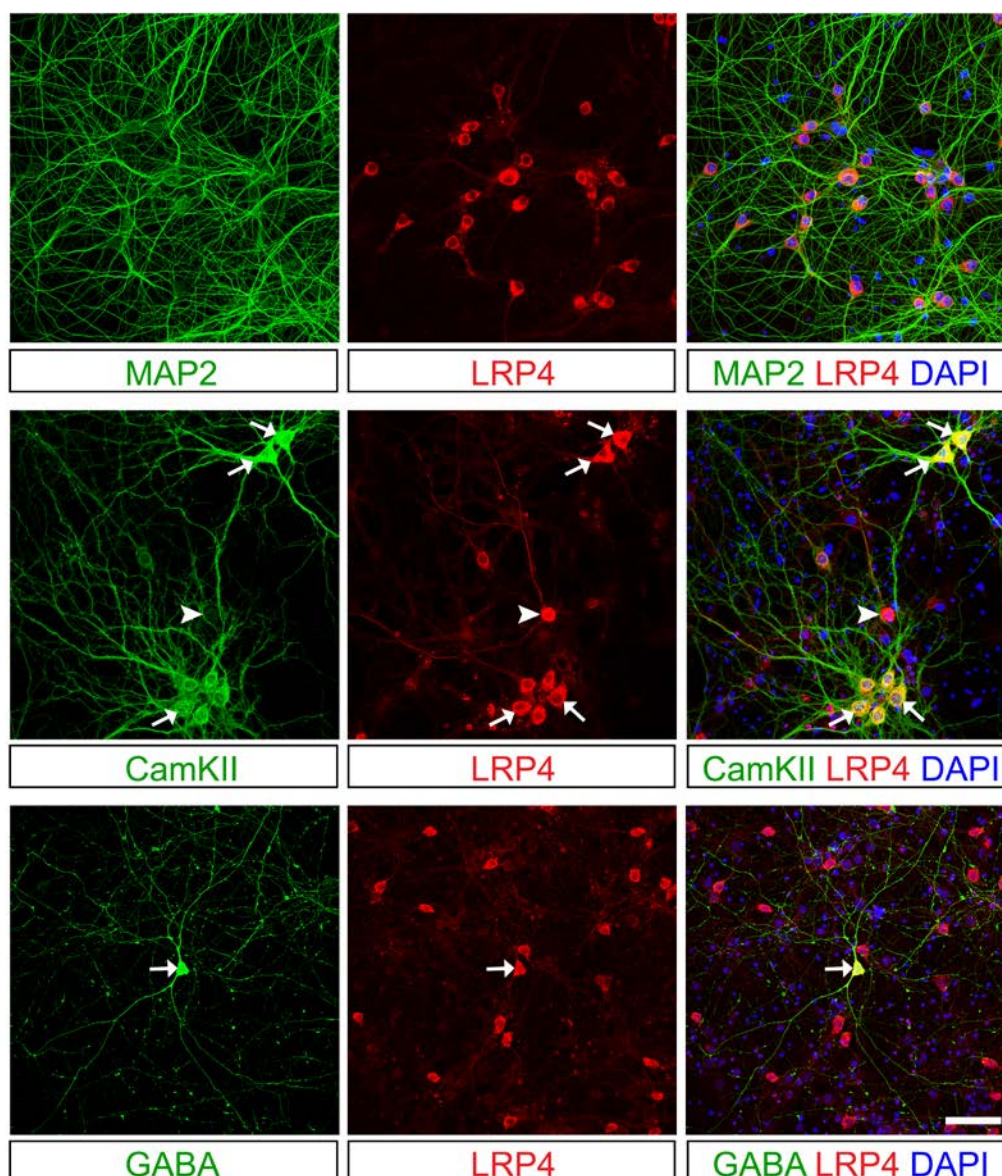
Cultures were placed in a recording chamber and superfused (1 mL / min) with artificial cerebrospinal fluid solution (in mM): NaCl, 125; KCl, 2.5; NaHCO<sub>3</sub>, 25; CaCl<sub>2</sub>, 2; MgCl<sub>2</sub>, 1; NaH<sub>2</sub>PO<sub>4</sub> 1.25 and glucose 25, saturated with 5% CO<sub>2</sub> and 95% O<sub>2</sub>, pH 7.4. Experiments were performed at 30-32 °C. Patch-clamp whole-cell recordings were obtained with electrodes fabricated from thick borosilicate glasses

pulled to a final resistance of 5–10 M $\Omega$  and filled with (in mM): K-gluconate, 125; NaCl, 5; Na<sub>2</sub>-ATP, 2; MgCl<sub>2</sub>, 2; EGTA, 10; HEPES, 10; biocytin, 10; pH 7.4. Transduced neurons were visually identified by fluorescence (GFP/Cy3 fluorescence optics; Axio Imager 2, Zeiss, Germany) and bright field videomicroscopy. Voltage-clamp recordings were obtained using Axopatch 200B (Molecular Devices), digitized (Digidata 1440a, Molecular Devices), and acquired using the pClamp 10 software (Molecular Devices). Seal resistances were between 4 and 18 G $\Omega$ . Spontaneous miniature excitatory postsynaptic currents (mEPSC) were recorded for 180 sec. at a holding potential of -70 mV in the presence of 0.5  $\mu$ M tetrodotoxin (TTX, Tocris). Data analysis was performed off-line using Clampfit 10 (pClamp 10, Molecular Devices).

#### SUPPLEMENTARY REFERENCES

- Choi, H. Y., Liu, Y., Tennert, C., Sugiura, Y., Karakatsani, A., Kroger, S., Johnson, E. B., Hammer, R. E., Lin, W. and Herz, J.** (2013). APP interacts with LRP4 and agrin to coordinate the development of the neuromuscular junction in mice. *eLife* **2**, e00220.
- Costa, M. R., Ortega, F., Brill, M. S., Beckervordersandforth, R., Petrone, C., Schroeder, T., Gotz, M. and Berninger, B.** (2011). Continuous live imaging of adult neural stem cell division and lineage progression in vitro. *Development* **138**, 1057-1068.
- Eusebio, A., Oliveri, F., Barzaghi, P. and Rugg, M. A.** (2003). Expression of mouse agrin in normal, denervated and dystrophic muscle. *Neuromuscular disorders : NMD* **13**, 408-415.
- Longair, M. H., Baker, D. A. and Armstrong, J. D.** (2011). Simple Neurite Tracer: open source software for reconstruction, visualization and analysis of neuronal processes. *Bioinformatics* **27**, 2453-2454.
- Zhang, Y., Lin, S., Karakatsani, A., Rugg, M. A. and Kroger, S.** (2015). Differential regulation of AChR clustering in the polar and equatorial region of murine muscle spindles. *The European journal of neuroscience* **41**, 69-78.

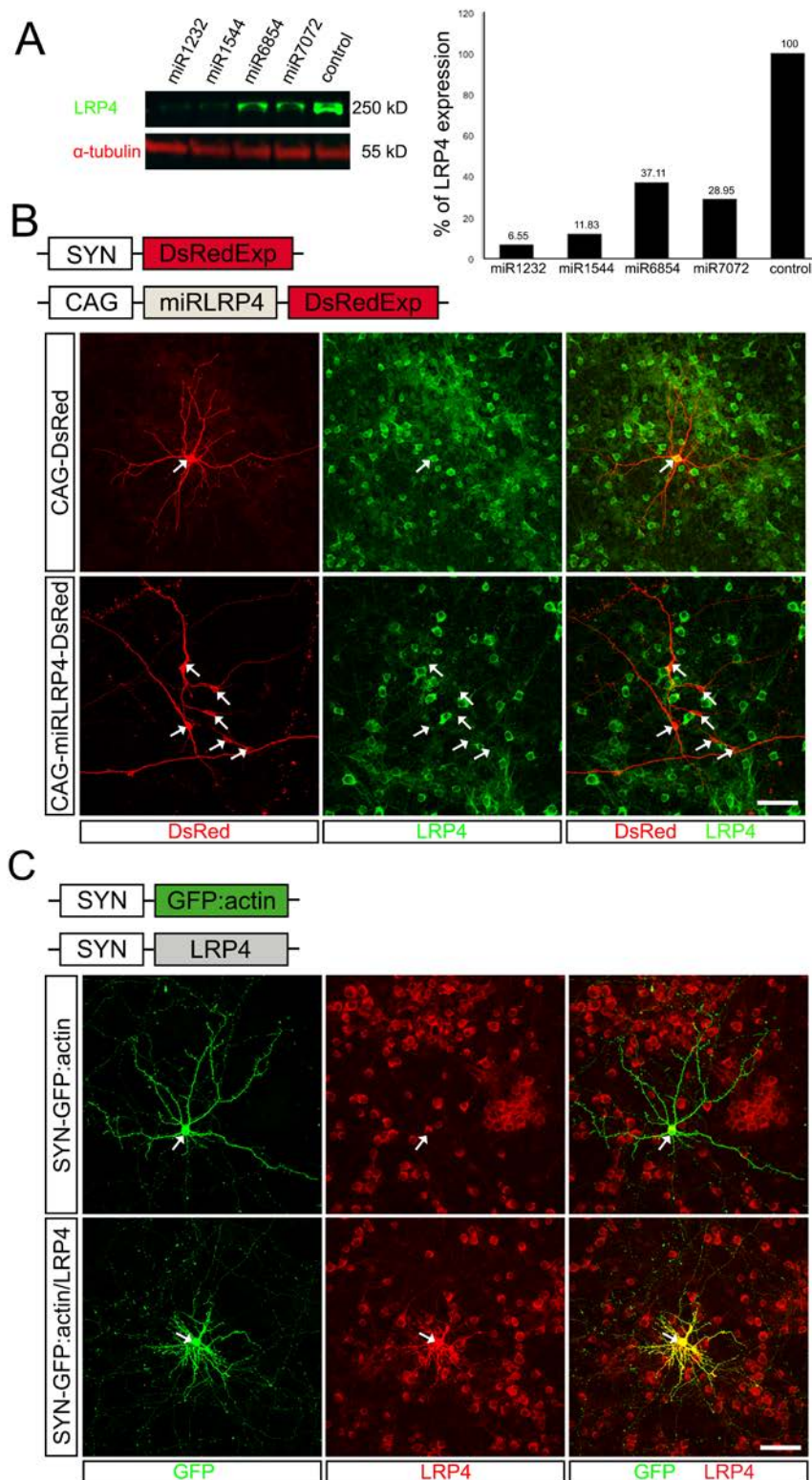
## SUPPLEMENTARY FIGURES



### Supplementary Figure 1

#### **LRP4 expression in cultures from embryonic hippocampus**

Dissociated cells from the E16 hippocampus fixed on DIV12 and labeled for LRP4, MAP2,  $\alpha$ -CamKII or GABA, respectively. Note that LRP4 is localized in both CamKII positive (arrows in middle panel of pictures) and GABA positive neurons (arrowhead in middle panel and arrow in lower panel of pictures). Nuclei were labeled with DAPI. Scale bar: 50  $\mu$ m.

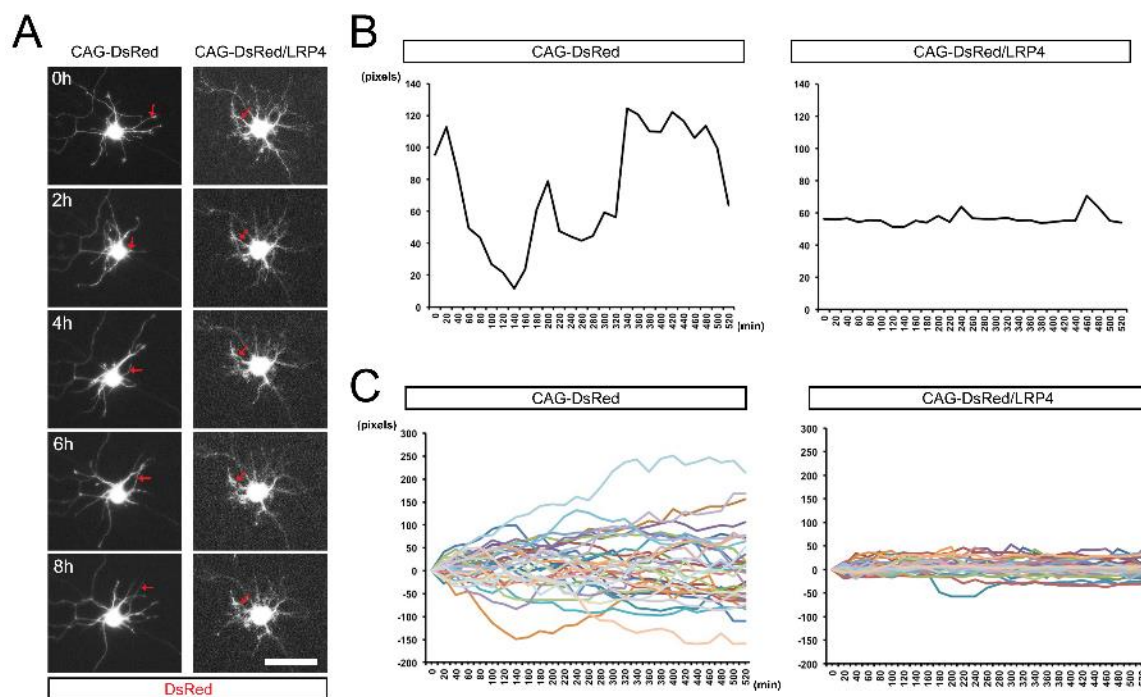


**Supplementary Figure 2**

**Characterization of constructs for overexpression and knockdown of LRP4**

(A) Analysis of the knockdown efficiencies of the four microRNAs (miR1232, miR1544, miR6854 and miR7072). HEK293 cells were co-transfected with pCMV-

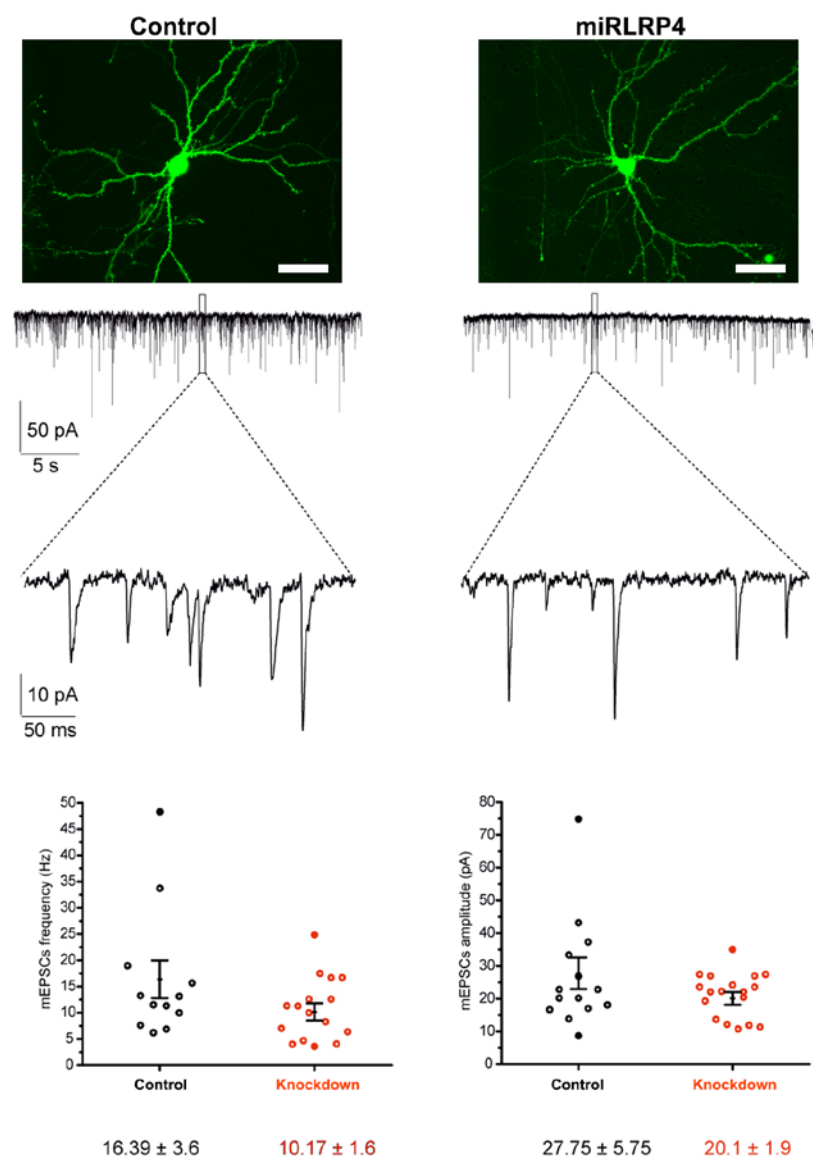
LRP4 and either the microRNA plasmids or the control microRNA. Proteins were harvested 48 hr post-transfection and separated using SDS-polyacrylamide gel electrophoresis followed by Western blotting. Equal loading of the lanes was controlled by probing the blot with anti-tubulin antibodies shown in red. The right panel shows the quantification of the LRP4 protein levels in HEK293 cells using fluorescently labeled secondary antibodies and the LiCor quantification system. Note that miR1232 and miR1544 reduce LRP4 levels with an efficiency of approximately 95% and 90%, respectively. Therefore these two miRNAs were used in all subsequent experiments. (B) Constructs encoding DsRed and miRLRP4 (miR1232 and miR1544 in tandem array) used to reduce LRP4 expression *in vitro* and *in vivo*. DsRed and miRLRP4 expression were under the control of the CAG promoter. Representative examples of dissociated cells from the E14 cerebral cortex transfected with pCAG-miRLRP4-DsRed or the empty pCAG-DsRed vector as control. Transfection with the empty pCAG-DsRed does not alter the levels of LRP4 (arrow in upper panels). In contrast, transfection with the pCAG-miRLRP4-DsRed plasmid strongly reduced the LRP4 levels in cortical neurons (arrows in lower panels). (C) Constructs for expression of GFP:actin and LRP4 transgenes. Representative examples of dissociated cells from the E16 hippocampus at DIV10 transfected with pSYN-GFP:actin and pSYN-LRP4 (lower panels) or the empty pSYN-GFP:actin plasmid as control (upper panels). Note the robust immunostaining for LRP4 in neurons after transfection with the pSYN-LRP4 vector (arrow in the lower panels) compared to its endogenous levels when transfected with the control plasmid (arrow in the upper panels). Scale bars: 50  $\mu$ m (B and C).



### Supplementary Figure 3

#### Overexpression of LRP4 in cultured cortical neurons reduces the dynamics of primary dendritic growth

(A) Fluorescence micrographs of representative examples of neurons from the E14 cerebral cortex (DIV5-6) co-transfected with pCAG-DsRed and pSYN-LRP4 or the empty pCAG-DsRed control vector and live-imaged for 8 hours two days after transfection. Red arrows indicate single dendritic processes followed over the imaging time. (B) Graphs representing the mobility of the two dendrites indicated by red arrows in panel A. The x axis represents the time in minutes and the y axis represents the length of each dendrite (2.016 pixels/ $\mu\text{m}$ ). While dendrites of neurons transfected with the control vector are highly dynamic, overexpression of LRP4 results in an absence of motility and a stop of dendrite growth. (C) Overlay of the motility analysis of 35 (control) and 37 (overexpression) dendritic processes from 3 independent experiments. Note that some dendrites decrease in length while the majority increases whereas after LRP4 overexpression, neither shrinkage nor growth was observed. Scale bar: 50  $\mu\text{m}$  (A).

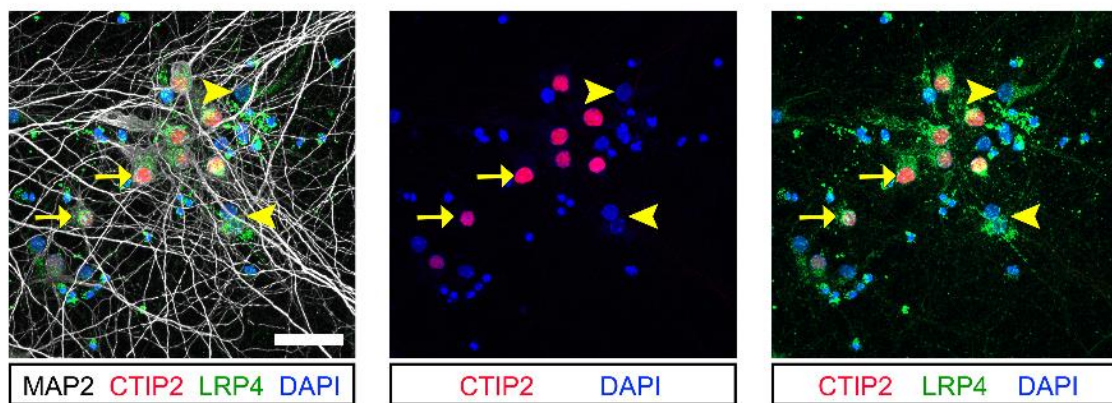


#### **Supplementary Figure 4**

#### **Neuronal spontaneous miniature excitatory postsynaptic currents upon LRP4 knockdown**

(A) Epifluorescence images of cultured hippocampal neurons recorded (left, control, right, knockdown). (B) Representative whole-cell voltage-clamp traces of mEPSC recorded at -70 mV in control (left) and knockdown (right) neurons. Recordings were obtained in the presence of TTX (0.5  $\mu$ M). Top, Time-compressed traces. Bottom, Expanded traces showing individual events. (C) Frequencies (measured during 60 s) and amplitudes (presented as mean value for each cell) of mEPSC events. Differences between control and knockdown neurons showed a trend, but were not statistically significant ( $p=0.11184$  frequency,  $p=0.39532$  amplitude, Mann-Whitney U Test). Black lines indicate mean  $\pm$  SEM.

Hippocampal neurons (DIV14)



**Supplementary Figure 5**

**Co-expression of LRP4 and CTIP2 in cultured hippocampal neurons.** Dissociated cells from the E16 hippocampus fixed on DIV14 and labeled for LRP4, MAP2 and CTIP2. Note that LRP4 is localized in both CTIP2 positive (yellow arrows) and CTIP2 negative neurons (yellow arrowheads). Nuclei were labeled with DAPI. Scale bar: 50  $\mu$ m.